

DURABILITY EVALUATION OF SURFACE SOFTENED STEEL BAR FOR PRESTRESSED CONCRETE

KENGO IWANAGA^{a,*}, SHIGERU MIZOGUCHI^b, YU MATSUMOTO^c,
KENICHI TAKAI^d, MIKIYUKI ICHIBA^e

^a Neturen Czech s.r.o., Jizni 1079 Bitovezes Prumyslova zona Triangle 438 01 Bitovezes Czech Republic

^b Neturen Co., Ltd., 2-17-1 Higashi-Gotanda, Shinagawa-ku, Tokyo 141-8639, Japan

^c Sophia University, 7-1 Kioi-cho, Chiyoda-ku, Tokyo 102-8554, Japan

^d Department of Engineering and Applied Science, Faculty of Science and Technology, Sophia University, 7-1 Kioi-cho, Chiyoda-ku, Tokyo 102-8554, Japan

^e R&D dept., Tokyo Electric Power Company Holding, Inc., 4-1 Egasaki-cho, Tsurumi-ku, Yokohama 230-8510, Japan

* corresponding author: k-iwanaga@neturen-czech.com

ABSTRACT. The effects of Si addition and surface softening on delayed fracture susceptibility were evaluated in tempered martensitic steels with tensile strength of 1450 MPa. The delayed fracture susceptibility was reduced when Si content was increased from 0.2 mass% to 1.88 mass%. The delayed fracture susceptibility of steel containing 1.88 mass% Si was reduced further when the tensile strength of its surface was lowered to around 1150MPa. Based on above results, the durability of these steel bars was evaluated by exposure test of prestressed concrete poles (CP). The bending load of the PC pole was 1.3 times of the design load. As a result of dismantling investigation after 10 years exposure test, there were no breakage of the steel bars in the PC poles and the soundness was maintained. In this paper, we will also introduce some comparison results of exposure tests and acceleration tests with aiming to establish the evaluation methods for the long-term durability.

KEYWORDS: Delayed fracture, durability, prestressed concrete pole, surface softened steel bar.

1. INTRODUCTION

In recent years, due to the arising problems of climate change and resources depletion, sustainable social and economic activities are being pursued. One of the basis of such social and economic activities is construction works, which requires huge amount of natural resources as well as energy, and this usage is estimated to increase in coming years. In this study, we aimed at the following two purposes.

1. Manufacture of high-strength, high-durability "prestressed concrete" (hereinafter referred to as PC) steel bar by "high-frequency induction heating quenching and tempering" (hereinafter referred to as IQT) with low CO₂ emissions.
2. Reducing lifetime costs by using this PC steel bar to improve the durability and safety of buildings. The IQT-type PC steel bar was developed in 1956 and has since been in use until today [1], but there is concern about delayed fracture, and overcoming it is an issue for improving durability.

It is known that the following two points are the basic ideas for improving durability against delayed fracture [2].

1. Suppression of the "hydrogen concentration from the environment" (hereinafter referred to as "He") that intrudes into PC steel bar.

2. Increasing the "critical hydrogen concentration which causes fracture" (hereinafter referred to as "Hc") in PC steel bar.

Based on this viewpoint and aiming for the improvement in the delayed fracture durability, optimized of chemical composition for high temperature tempering as well as developed surface softening tempering treatment. The developed IQT type 1420MPa class PC steel bar has the same mechanical properties as the conventional material and has remarkably excellent durability against delayed fracture [3].

The PC steel used in this study was evaluated by various delayed fracture evaluation methods [4], and the mechanism for improving its delayed fracture was discussed. Furthermore, it was subjected to an exposure test using a "concrete pole" (hereinafter referred to as "CP") as specimens using the developed PC steel bar. The CPs which had been exposed for more than 10 years were investigated and their durability was examined in terms of the effects of damage and the possibility of delayed fracture.

2. EXPERIMENTAL PROCEDURE

2.1. CHEMICAL COMPOSITION OF MATERIALS

The materials used in this study are IQT type PC steel bars which are manufactured according to JIS

	C	Si	Mn	P	S	Cu	Ti	B
JIS G3137	-	-	-	≤ 0.030	≤ 0.035	≤ 0.03	-	-
IQT-C _{onventional}	0.30	0.21	0.72	0.019	0.002	0.01	0.03	0.0016
IQT-I _{mproved}	0.32	1.80	0.74	0.018	0.005	0.01	0.04	0.0023
IQT-S _{urface softening}								

TABLE 1. Chemical composition of test materials(mass%).

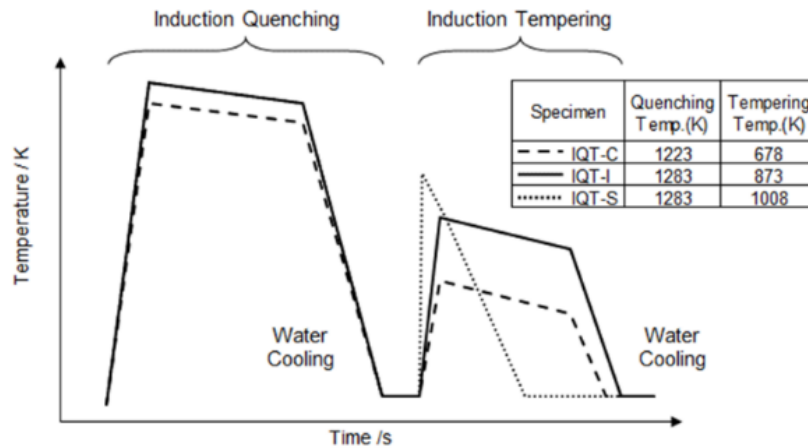


FIGURE 1. Schematic diagram of heat-treating cycle of IQT-C, IQT-I and IQT-S.

Specimen	0.2% Proof Strength [N/mm ²]	Tensile strength [N/mm ²]	Elongation [%]	Uniform Elongation [%]	Reduction of Area [%]
JIS G3137	≥1275	≥1420	≥5	-	-
IQT-C	1316	1426	8.5	1.8	67
IQT-I	1430	1458	12.9	4.6	68
IQT-S	1396	1448	12.3	3.8	65

TABLE 2. Mechanical Properties.

G3137 (small diameter steel bar for prestressed concrete). Table 1 shows the chemical composition of conventional material (IQT-C), improved material (IQT-I) and improved material with surface-softening temper treated (IQT-S). With the aim of increasing the tempering temperature, the composition of Si is increased in improved materials, contributing to increase in resistance towards softened due to tempering.

2.2. MANUFACTURING METHODS

Rolled wire rods with chemical composition shown in Table 1 were shaped by deformed wire drawing process and subjected to continuous high frequency induction quenching and tempering. By increasing the amount of Si compared to IQT-C, the maximum tempering temperature for IQT-I was able to be raised until 880 K. The surface-softening tempering process was conducted for IQT-S using the same equipment as to IQT-I, in which the material was first subjected to high temperature and short time tempering and then the cooling time was adjusted so that the rate of tempering progression throughout the materials sur-

face was maximized. It was possible for the maximum tempering temperature of this material to reach until 1028 K. The schematic diagram for the heat treatment cycles are shown in Figure 1.

2.3. MECHANICAL PROPERTIES

The mechanical properties for the materials are shown in Table 2. The tensile properties were measured in accordance with JIS G3137. The tensile strengths for IQT-C, IQT-I and IQT-S are almost the same and their mechanical properties satisfy JIS G3137. Figure 2 shows the measurement result of Vickers hardness from the surface to the core in radial direction as well as tensile strength calculated from the Vickers hardness. There are relatively no changes in the hardness from the surface to the core of IQT-C and IQT-I. The Vickers hardness for IQT-S gradually increases from 350 HV at the outermost surface towards the same hardness as common IQT material at around 1 mm from the outermost surface. Then, the hardness remains relatively unchanged at 1.5 mm from the surface until the core.

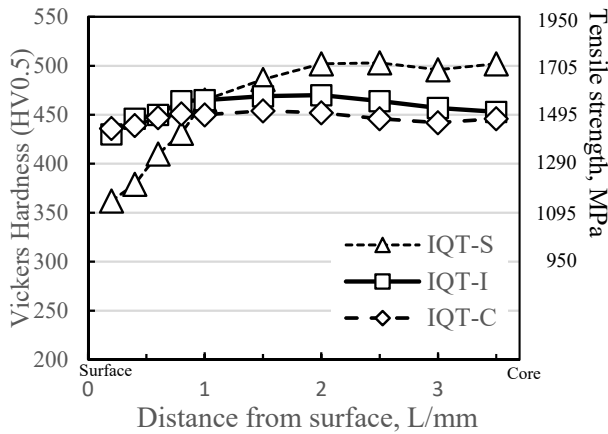


FIGURE 2. Vickers hardness from the surface to the core of IQT-C, IQT-I and IQT-S.

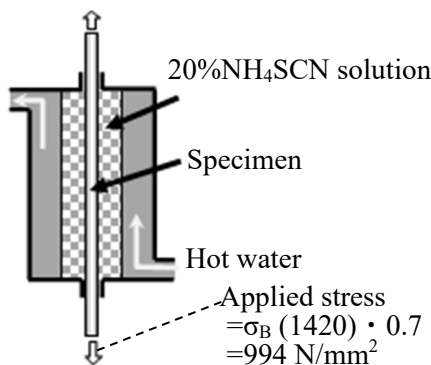


FIGURE 3. Schematic diagram of FIP test method.

2.4. MICROSTRUCTURE AND FRACTURE SURFACE

During preparation for the microstructure observation, the specimens were first cut using wet whetstone cutter then the cut sections were mirror polished and subsequently etched using 3% nital etching solution to clarify the microstructure. The microstructures of materials were observed using optical microscope or scanning electron microscope (SEM). The materials were machined into thin film specimens and used for observation of carbides precipitation using transmission electron microscope (TEM). The fracture surfaces were cleaned using adhesion tape or ammonium citrate depending on necessity before being observed on SEM.

2.5. DELAYED FRACTURE DURABILITY EVALUATION TEST

2.5.1. FIP (FÉDÉRATION INTERNATIONALE DE LA PRÉCONTRAÎNTE) TEST-1980

To increase the reproducibility of FIP test which was endorsed by FIP in 1980, tests were conducted according to "Method of hydrogen embrittlement test for steel for pre-stressed concrete in a 20% ammonium thiocyanate solution" (JSCE S 1201) established in 2012 by Japan Society of Corrosion Engineering [5].

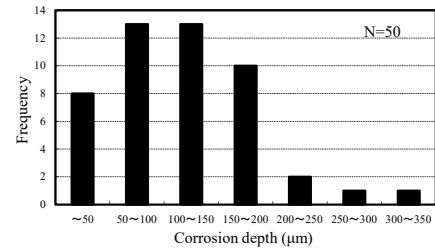


FIGURE 4. Pitting corrosion depth distribution of tendon in CP after completion of service.

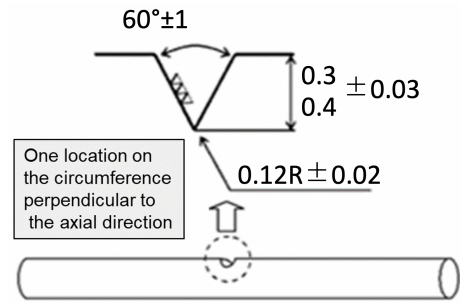


FIGURE 5. V-notch shape of specimen.

Figure 3 shows the schematic diagram of FIP test. To maintain the temperature inside the reaction cell at 323 ± 1 K, test containers equipped with hot water circulation were used in the test. The reaction cell was filled with 20% NH_4SCN aqueous solution at 323 K and smooth bar specimen is set up so that it passed through the cell. Hydrogen entry into the specimen occurs due to chemical reaction between the specimen's surface and the test solution. The test was conducted in a way where the reaction cell was firstly filled up with test solution and then immediately tension stress of 0.7 times of standard strength ($1420 \times 0.7 = 994 \text{ N/mm}^2$) was applied to the specimen. The time until fracture was measured and test was stopped at 200 h even when no fracture occurs.

2.5.2. CRITICAL DIFFUSIBLE HYDROGEN MEASUREMENT

Figure 4 shows the corrosion pits depth distribution of tendon in CP after completion of service. The maximum depth of corrosion pit measured is about $350 \mu\text{m}$. V-notches of depth 0.3 mm or 0.4 mm were applied on the specimens to model the corrosion pits found in service materials. The radius of the notch tip where stress concentration occurs was machined to 0.12 mm for evaluation of materials with harsher condition than the ones in service environment. The dimensions of the specimen are shown in Figure 5.

Delayed fracture tests with continuous hydrogen charging of the V-notched specimens in different concentrations of NH_4SCN solution at 323 K were conducted using 2 conditions stated below. Assuming a condition in which corrosion pits occur under normal tension load in "slightly harsh environment" condition, load stress of 0.7 times the magnitude of tensile



FIGURE 6. Exposure test of "CP500" utility poles at the Choshi test site in Japan (started in August 2010).



FIGURE 7. Exposure test of "CP350" utility poles at the Muroran test site in Japan (started in July 2013).

strength was applied towards specimens with notch depth of 0.3mm. Meanwhile, in "harsh environment" condition, load stress of 0.85 times the magnitude of tensile strength was applied towards specimens with notch depth of 0.4 mm to assumptive a condition in which corrosion pits with maximum depth as well as load higher than the limit CP in service. The maximum concentration of NH_4SCN solution during which no fracture occurs in 100 h test time is determined. Different specimens than the ones in delayed fracture tests are immersed for 100 h in NH_4SCN solutions of concentration determined earlier and then the diffusible hydrogen concentration measured using thermal desorption method from room temperature to 573 K is classified as Hc.

2.5.3. CP EXPOSURE TEST

Following JIS A5364 and JIS A5373, CP (CP500) with length 14 m and design load 4.9kN as well as CP (CP350) with length 13 m and design load 3.4kN were manufactured using IQT-C and IQT-S. The specifications of the arrangement of PC steel bar are same as to the ones used in real utility poles.

CP500 were set up at Choshi, Chiba in Japan (About 4km from southern coast) and exposure tests were started from August of 2010. The tests were set up such that design load (4.9kN) which is the instantaneous abnormal high load such as from typhoon, as well as 1.2 times the design load (5.9kN) were always applied towards the horizontal direction of the CP's upper part. Figure 6 shows the condition of the exposure tests. CP350 were set up at Muroran, Hokkaido in Japan (About 20 m from sea) and exposure tests were started from July of 2013 by always application of design load (3.4kN) or 1.3 times the design load(4.4kN) in the horizontal direction of the upper part of the CP. The tests condition is shown in Figure 7.

3. RESULTS

3.1. DELAYED FRACTURE DURABILITY EVALUATION RESULTS

3.1.1. FIP TEST RESULT

Figure 8 shows the result of FIP test. Each data was sorted using Mean Rank Method and then cumulative failure probability was calculated and presented as lognormal probability plot. At 50% cumulative failure probability, fracture is recorded at 18.8 h for IQT-C, while no fracture is recorded at stop time of 200 h for IQT-I which has higher Si composition. Moreover, surface-softening tempered IQT-S also experiences no fracture at 200 h, showing substantial improvement in delayed fracture durability that is not possible to be evaluated by FIP test alone.

3.1.2. CRITICAL DIFFUSIBLE HYDROGEN (Hc) MEASUREMENT RESULT

The concentration of hydrogen that enters from environment (He) is found to be around 0.15 ppm from previous research [6] and it is suggested that the higher Hc is from 0.15 ppm, the better the durability of the material against delayed fracture. Figure 9 shows the measurement result of Hc. In "slightly harsh environment" condition (0.3 mm Notch- $0.7\sigma_B$), Hc was higher than He regardless of the types of material. However, in "harsh environment" condition (0.4 mm Notch- $0.85\sigma_B$) Hc decreased until below 60 percent than that of in "slightly harsh environments" and Hc from IQT-C became smaller than He. Regardless of the environment model, the pattern for Hc was $\text{IQT-C} < \text{IQT-I} < \text{IQT-S}$. The effectiveness of the methods for improving durability against delayed fracture was confirmed from this result.

3.2. CP EXPOSURE TEST RESULTS

3.2.1. CP500 CHOSHI EXPOSURE TEST

Figure 10 shows the crack width measurement result of the cracks found on the surface of CP at the third

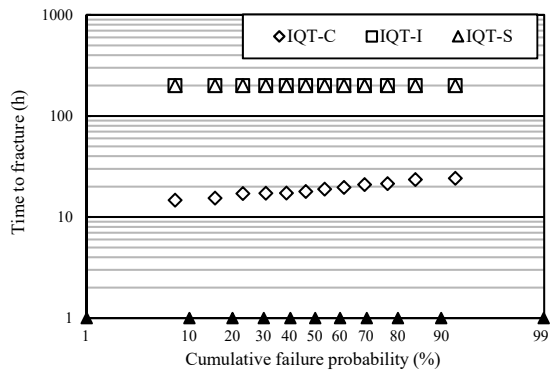


FIGURE 8. Delayed fracture resistance evaluation using quasi-FIP test.

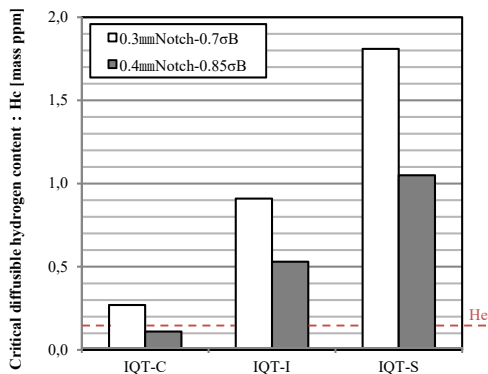


FIGURE 9. Measurement result of critical diffusible hydrogen (Hc) without delayed fracture after 100 h.

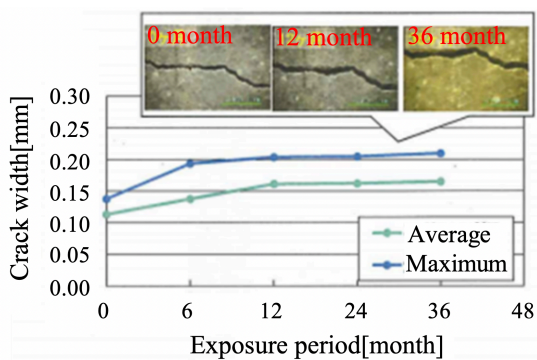


FIGURE 10. Crack width measurement result of CP500 utility poles using IQT-S as tendon.

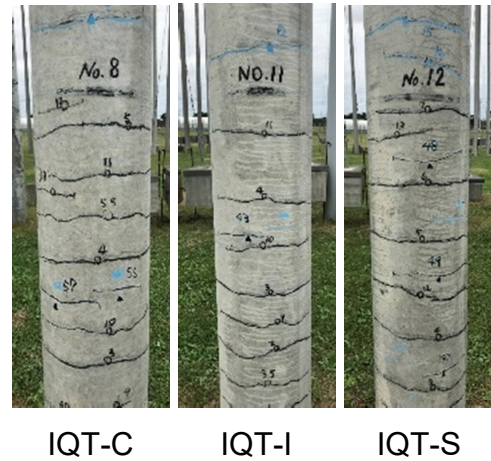


FIGURE 11. Results of external observation of CP500 utility poles exposed to bending for 5.9kN for 10 years.

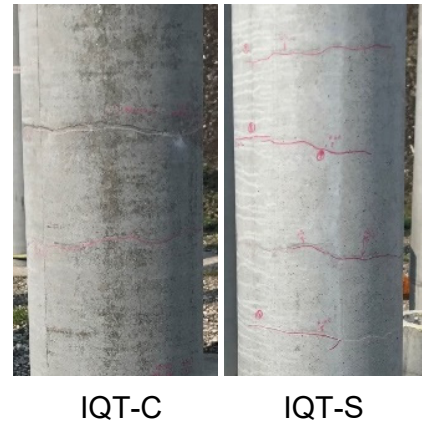


FIGURE 12. Results of external observation of CP350 utility poles exposed to bending for 4.4kN for 5 years.

year of exposure test. The cracks occurred immediately after load application and expanded until as large as 0.2 mm at around the first year. It was observed that the cracks' enlargement slowed down following the first year. Figure 11 shows the external observation of utility poles after 10 years of exposure test. The result of using leakage magnetic flux method to detect any fracture in the steels shows that there were no major abnormalities nor any fractures detected for all IQT-C, IQT-I and IQT-S. Thus, the exposure test is still ongoing in the present time.

3.2.2. CP350 MURORAN EXPOSURE TEST

Figure 12 shows the results of external observation of IQT-C and IQT-S utility poles after 5 years of exposure test. Several cracks were found on the surface of CP. The cracks were after enlargement until about 0.2 mm, there were no remarkable changes in the width of cracks on the CP surface. There was no fracture detected by using leakage magnetic flux method at the fifth year of exposure test. The IQT-C and IQT-S utility poles were dismantled and the condition of

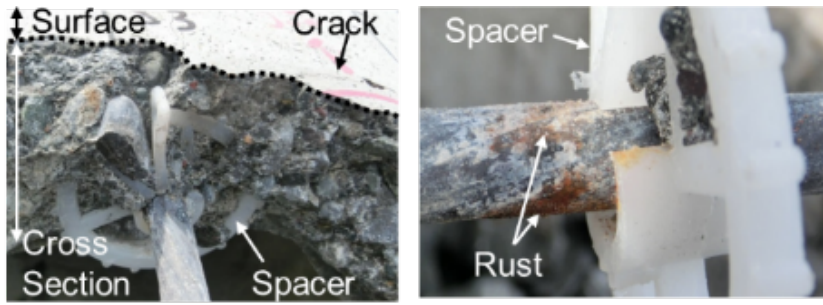


FIGURE 13. Observation results of cracks and spacers during dismantling of the utility pole.



FIGURE 14. Observation of corrosion state of PC steel bar at the joint position of the concrete formwork during dismantling CP.

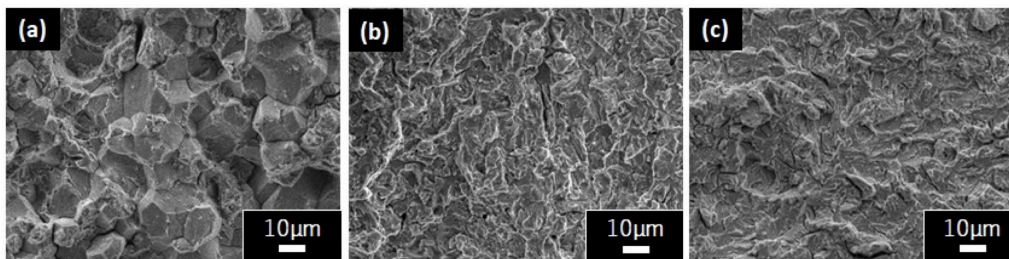


FIGURE 15. Microscopic fracture surfaces near the notch tip after delayed fracture test; (a) a IQT-C specimen shows intergranular (IG) fracture, (b) a IQT-I specimen shows quasi-cleavage (QC) fracture and (c) a IQT-S specimen also shows quasi-cleavage (QC) fracture.

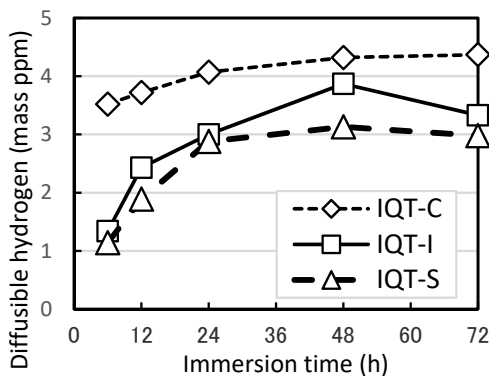


FIGURE 16. Relationship between immersion time and diffusible hydrogen content in 323 K-20% NH_4SCN solution.

fracture, cracks as well as rusts of the steel parts was examined. After dismantling, it was found that no fracture occurred in the PC steel bars of both utility poles. Figure 13 and Figure 14 show some examples of the crack parts during dismantling of the utility

poles. Local rusts were spotted on the surface of the steel bar located directly under the cracks. Several cracks were located in the vicinity of the areas where the bond strength is weak between the reinforcing bar and the concrete due to locally no contact existing between them, such as at the spacers put before the pouring of concrete into the formwork. Rusts also observed along the longitudinal direction of the formwork joints position of CP where is tends to low density concrete by centrifugal molding method.

4. DISCUSSION

4.1. THE MECHANISMS OF IMPROVEMENT OF DELAYED FRACTURE DURABILITY

4.1.1. EFFECTS OF ADDING Si AND B

Previous results show that the delayed fracture durability in IQT-I and IQT-S has improved compared to IQT-C, and the reasons are as follows.

Figure 15 shows the observation results of the fracture surfaces from the materials. Intergranular fracture was observed in IQT-C which has short time to

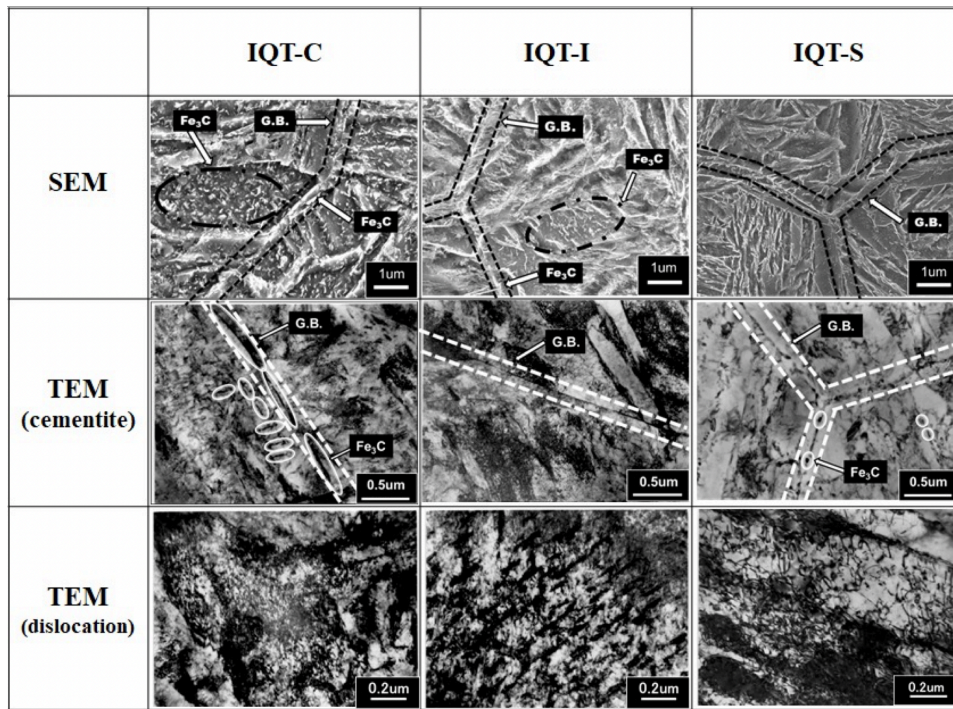


FIGURE 17. Microstructures of specimens obtained by a scanning electron microscopy and a transmission electron microscopy. The micrographs of IQT-S specimen are observed in surface-softened area at 0.4 mm apart from the surface.



FIGURE 18. Observation results of steel mark in concrete test piece after neutralization test.

fracture in FIP tests as well as small H_c . Meanwhile, intergranular fracture was not observed in IQT-I and IQT-S in which the composition of Si in the materials was increased. This correlates to the effects of Si in suppressing the formation of intergranular fracture as reported by previous study [7]. It is also thought that the addition of B in the materials suppressed the formation of intergranular fracture due to the effects of B in increasing the strength of grain boundaries as reported before [8].

4.2. EFFECTS OF SURFACE-SOFTENING TEMPERING

The results in 3.1.2 show that H_c for IQT-S is remarkably higher than IQT-I even though IQT-S is just a surface softening tempered IQT-I. The reasons for the increase of H_c for IQT-S despite having the same chemical composition and tensile strength are

as follows. Figure 16 shows the relationship between immersion time and diffusible hydrogen content when the specimens were immersed in 20% NH_4SCN solution. The rate of hydrogen diffusion is in the order of $IQT-S < IQT-I < IQT-C$.

As the rate of hydrogen diffusion in IQT-S is slower than IQT-I, this indicates that the surface-softening layer has certain resistance towards hydrogen entry into the material. In order to investigate this point, SEM and TEM observations of the microstructures of each material were conducted, and the results are shown in Figure 17. The observation results are summarized in order of increasing tempering temperature (IQT-C, IQT-I, IQT-S) as follows.

1. As the tempering temperature increases, the carbide precipitations become smaller and the precipitation sites change from the grain boundaries to the inner grain parts. These are also the characteristics of materials that have undergone high frequency induction tempering (short time heating).
2. As the tempering temperature increases, the shape of the carbide precipitated on the grain boundaries changes from plate-shape to film-shape and lastly to divided sphere-shape.
3. The areas with high dislocation density are shown as black contrast areas in the TEM observation results. As the tempering temperature increases, the white areas which represented areas with low dislocation density increase, confirming the progression of tempering.

Hydrogen diffusion is closely related to the dislocation motion in materials. As such, the amount of hydrogen transported from the steel surface into the inner matrix increases when dislocations become more mobile or dislocation densities increase. Therefore, the amount of diffusible hydrogen decreases because the fine distribution of carbides into the inner grain hinders the dislocation mobility as well as the dislocation densities decrease.

Based on the observation results above, it is conjectured that the main focus for the mechanisms of the delayed fracture durability improvement lies on the high temperature and short time tempering which is possible due to Si addition and surface-softening tempering. The process transforms the coarse plate-shape carbides on the grain boundaries into fine sphere-shape carbides, which results in the increase of grain boundaries strength as well as suppressing the hydrogen diffusion through dislocation.

4.3. IMPROVEMENT OF THE DURABILITY OF CP

In this section the factors behind no fractures occurring for IQT-C and IQT-S reinforcement bars at the CP350 Murooran exposure test are discussed. After dismantling of CP350, neutralization test using phenolphthalein was conducted towards the concrete parts which included the crack parts. Figure 18 shows one example of the test results. The observed surface changed pink colour which indicated that neutralization did not occur whether on the crack part nor the steel mark part. Thus, it can be inferred that even though rusts form on the steel bars, since either the rust progression was slow or the corrosion environment was not sustained, entry of hydrogen exceeding Hc did not occur even in IQT-C with low Hc value. Furthermore, it should also be noted that the cold climate and low humidity at the Murooran test site may affect the corrosion's rate of progression and sustainability. However, fractures were also not recorded at the CP500 (Choshi test site) where it is warmer and more humid than Murooran. Thus, further plans for the verification of durability in real environment involve the continuation of tests while also recording environmental data.

5. CONCLUSIONS

High frequency induction quenched and tempered PC steel bars with improved durability were developed by increasing the tempering temperature due to Si addition, as well as conducting surface-softening tempering process. The use of this PC steel bars can be expected to improve PC durability.

CP were manufactured using these PC steel bars and subjected to excessive bending load while exposed to real environment. The results showed that no fracture occurred in both conventional material and improved material even for test that has been ongoing for 10 years.

With this, we will continue to strive in the future to reduce environmental loads and contribute to society through the development of high quality products utilizing technologies with little environmental loads such as high frequency induction heat treatment.

REFERENCES

- [1] M. Yamada. Recent Topics on Prestressing Steel. *Concrete journal Japan Concrete Institute*. **47**(11):3-8, 2009. http://www.jci-net.or.jp/j/publish/bulletin/e_pdf/e_outline_200911.pdf.
- [2] T. Tarui, M. Kubota. Approaches for Fundamental Principles 1: Method of Hydrogen Embrittlement and Improvement Techniques of Delayed Fracture, *Nippon Steel Technical Report* **391**(101):155-157, 2011. https://www.nipponsteel.com/en/tech/report/nsc/pdf/NSTR101-23_tech_review-3-4.pdf.
- [3] Y. Matsumoto, K. Takai, M. Ichiba, et al. Reduction of Delayed Fracture Susceptibility of Tempered Martensitic Steel through Increased Si Content and Surface Softening. *ISIJ International* **53**(4):714-22, 2013. <https://doi.org/10.2355/isijinternational.53.714>.
- [4] T. Tarui, S. Yamasaki. Evaluation Method of Delayed Fracture Property and Overcoming Techniques of Delayed Fracture of High Strength Steels. *Tetsu-to-Hagane* **88**(10):612-9, 2002. https://doi.org/10.2355/tetsutohagane1955.88.10_612.
- [5] JSCE S 1201-2012. Method of Hydrogen Embrittlement Test for Steel for Prestressed Concrete in a 20% Ammonium Thiocyanate Solution, JSCE, Tokyo, 2012.
- [6] T. Kushida. Hydrogen Entry into Steel by Atmospheric Corrosion. *ISIJ International* **43**(4):470-4, 2003. <https://doi.org/10.2355/isijinternational.43.470>.
- [7] R. Hobbs, L. GW. Effect of silicon on the microstructure of quenched and tempered medium-carbon steels. 1972.
- [8] Y. Ohno, H. Fuji, S. Sekino. Effect of B on Delayed Class High Fracture property of high strength steels. *Tetsu-to-Hagane* **83**:42-47, 1997.